

Utilizing PlanetScope SuperDove imagery and a random forest machine learning approach for LULC mapping in the Nariva Swamp

DEANESH RAMSEWAK*, MICKELL GUNNESSLAL, ARVIND JAGASSAR, ARTHUR POTTS

Centre for Maritime and Ocean Studies, The University of Trinidad and Tobago, Chaguaramas Campus, 962-968 Western Main Road, Chaguaramas, Carenage 110804, Trinidad and Tobago

* Email: deanesh.ramsewak@utt.edu.tt

ABSTRACT. The Nariva Swamp, the largest freshwater wetland in Trinidad and Tobago, is currently facing increasing pressure from physical development. This study detects and maps changes in the land use and land cover (LULC) of the Nariva Swamp by employing GPS-ground data, high-resolution satellite imagery and advanced image processing techniques in Google Earth Engine (GEE). An accurate, updated LULC map of the Nariva Swamp was developed using machine learning, high-resolution Planet SuperDove (PSB.SD) 3 m per pixel satellite imagery, and field data. The performance of random forest (RF), support vector machine (SVM) and classification and regression trees (CART) machine learning (ML) algorithms was assessed. The results indicated that the overall accuracy of the RF, SVM and CART classifiers were 90%, 85% and 85% respectively. While all three algorithms produced high accuracy outputs, the RF classifier outperformed both the CART and SVM classifiers. The RF classifier was most suited to the development of LULC maps for the Nariva Swamp. The 2024 LULC map was compared to a 2009 LULC map of the Nariva Swamp. The key changes noted were among the water, urban and mangrove classes. The random forest algorithm applied is regarded as the best for future studies in the Nariva Swamp region.

Keywords: land use and land cover, PlanetScope SuperDove, GEE, machine learning, random forest.

1. INTRODUCTION

Coastal wetlands contain ecosystems with high biodiversity and typically help to advance productivity between the sea and the land (Nie et al., 2023). These highly diverse areas cover more than 12,200 million hectares of the Earth's surface (Millán et al., 2021) and provide several invaluable ecosystem services. These include coastal protection, flood control and water purification in addition to having the capacity to act as wind breaks during storm surges and hurricanes (Murdiyarsa et al., 2015; Newton et al., 2020). Despite their importance, coastal wetland ecosystems continue to face a range of problems on a global scale. Habitat loss due to deforestation and urbanization is a significant concern as these areas have diminished in size in recent decades (Choi et al., 2022). Increased pressures from agriculture, urban expansion, climate change and alterations to hydrological cycles continue to exacerbate the problem and cause further loss of biodiversity (Martínez-Megías & Rico, 2022). South American and Caribbean countries rank third in wetland coverage, accounting for 15.8% of the total global coastal wetlands (Millán et al., 2021). In the Caribbean region in particular, coastal wetlands encounter similar challenges which threaten the

sustainability of these landscapes such as mangrove deforestation for development, pollution from agricultural runoff and increased vulnerability to hurricanes and sea level rise.

Coastal wetlands in Caribbean islands are usually constrained by development on one side and the ocean on the other (Lagomasino et al., 2019). While these ecosystems provide much needed protection to inland development, they are constantly under threat of degradation and deforestation to accommodate urban expansion. Climate change impacts, such as sea-level rise and more frequent and intense hurricanes, also pose a significant threat to these ecosystems (Soanes et al., 2021). Estimates suggest that a one-meter elevation in sea level could put into risk over 72% of the World's coastal wetlands (Millán et al., 2021), including many in the Caribbean region. The region's heightened vulnerability to climate change related events puts these ecosystems at an even higher risk, potentially leading to further degradation and loss (Lagomasino et al., 2019). Caribbean nations rely heavily on these ecosystems for coastal protection and their destruction can result in increased erosion and damage to the shoreline and the coastal communities (Lagomasino et al., 2019). This is already occurring in regions along the eastern coastline of

Trinidad in the vicinity of the Nariva Swamp.

The Nariva Swamp is the largest freshwater wetland in Trinidad and Tobago, providing various benefits to the surrounding areas, local communities and the adjacent Manzanilla beach, which is protected due to its proximity to the swamp's mangrove forests (Mahabir & Nurse, 2007). Urbanization, improper land use practices and climate change, have caused significant destruction and degradation along the Manzanilla coastline in recent years. Over the past few years several incidents of extensive damage to roads, houses and farms in the area have occurred. Unprecedented weather events in 2015 wreaked havoc on substantial portions of the primary road and resulted in the devastating flooding and destruction of numerous houses (Jalim, 2015). In 2018 and 2022 weather events of a similar scale inflicted further destruction along the Manzanilla coastline, including the main road, residential properties, and the decimation of livestock and crops belonging to numerous local farmers (Paul & Sambran, 2022). Much of this has been attributed to climate change and increases in greenhouse gases such as carbon dioxide (Mahabir & Nurse, 2007). As a result, the wetland ecosystem faces a significant risk to its sustainability from these extreme climatic occurrences (Darsan et al., 2013).

The geographical positioning of the wetland renders it susceptible to storms originating from the Atlantic, and the dangers are heightened by its minimal elevation (Darsan et al., 2013). Studies have shown that coastal erosion and storm surges possess the capacity to breach the protective beach barriers such as at Manzanilla, while the vulnerability to tsunamis further increases the potential impacts (Darsan et al., 2013). Preserving the integrity of the Nariva Swamp has become increasingly important, and requires immediate and meticulous management measures (Darsan et al., 2013). Presently, there is a deficiency in up-to-date, comprehensive, LULC information for the area as can be seen in the Management Plan for the Nariva Swamp Protected Area 2019-2029 (FAO, 2019). An essential component of remedying this involves ensuring that current updated LULC maps of the swamp are created to accurately identify the most extensively impacted regions and prioritize them for urgent intervention. The development of an updated LULC map for the swamp promises to yield a more extensive understanding of the changes in land use and land cover patterns occurring within the boundaries of the swamp and facilitate enhanced efficacy in management efforts for the area.

Land cover mapping has been used for decades to detect change in a variety of environments (Zhu et al., 2022). However, the need for such maps is becoming increasingly vital in policy development and sustainable management (Saah et al., 2019). Using a combination of remote sensing and field verification techniques, highly accurate LULC maps can be developed which can be reproduced on a regular basis (Manandhar et al., 2009). Over the years, a variety of classification methods and algorithms have been used to develop LULC maps. These techniques usually utilize machine learning (ML) algorithms that are selected based on the availability of data and the characteristics of the environment to be classified (Vizzari, 2022). With advancements in different remote sensing tools, LULC maps continue to be developed with increasing accuracy (Mashala et al., 2023). More recent studies have also explored the potential of using deep learning techniques for land use and land cover classification with varying levels of success (Olaf et al., 2015; Mahdianpari et al., 2018; Vali et al., 2020; Cecili et al., 2023). This approach, however, requires large amounts of labelled data for the development of a reliable, robust model and can require significant resources to execute (Digra et al., 2022). As a result, LULC mapping is still heavily reliant on the use of ML algorithms. Among the different algorithms used are several which have consistently produced reliable results and are considered the conventional standards (Patil & Panhalkar, 2023). These include random forest (RF), artificial neural network (ANN), fuzzy ARTMAP (FA), support vector machine (SVM) and classification and regression tree (CART) classifiers (Talukdar et al., 2020; Vizzari, 2022). In this study, RF, SVM and CART were selected to carry out the classification as previous studies have demonstrated that they were best suited to wetland ecosystems (Vizzari, 2022). The performance of a model can be evaluated in a number of ways, however, for this study, this was done using a confusion matrix accuracy assessment to determine the kappa coefficients, overall accuracy and producer's and user's accuracies serving as key performance metrics (Zhao et al., 2024). While all three classifiers selected can produce reliable LULC maps (Zhao et al., 2024), several factors can influence their accuracy including the LULC types within the study area and the spatial and spectral resolutions of the imagery used (Talukdar et al., 2020).

Landsat-8 and Sentinel-2 satellite imagery are commonly used due to their easy accessibility through Google Earth Engine (GEE) (Nandy et al., 2017; Loukika et al., 2021). PlanetScope satellite

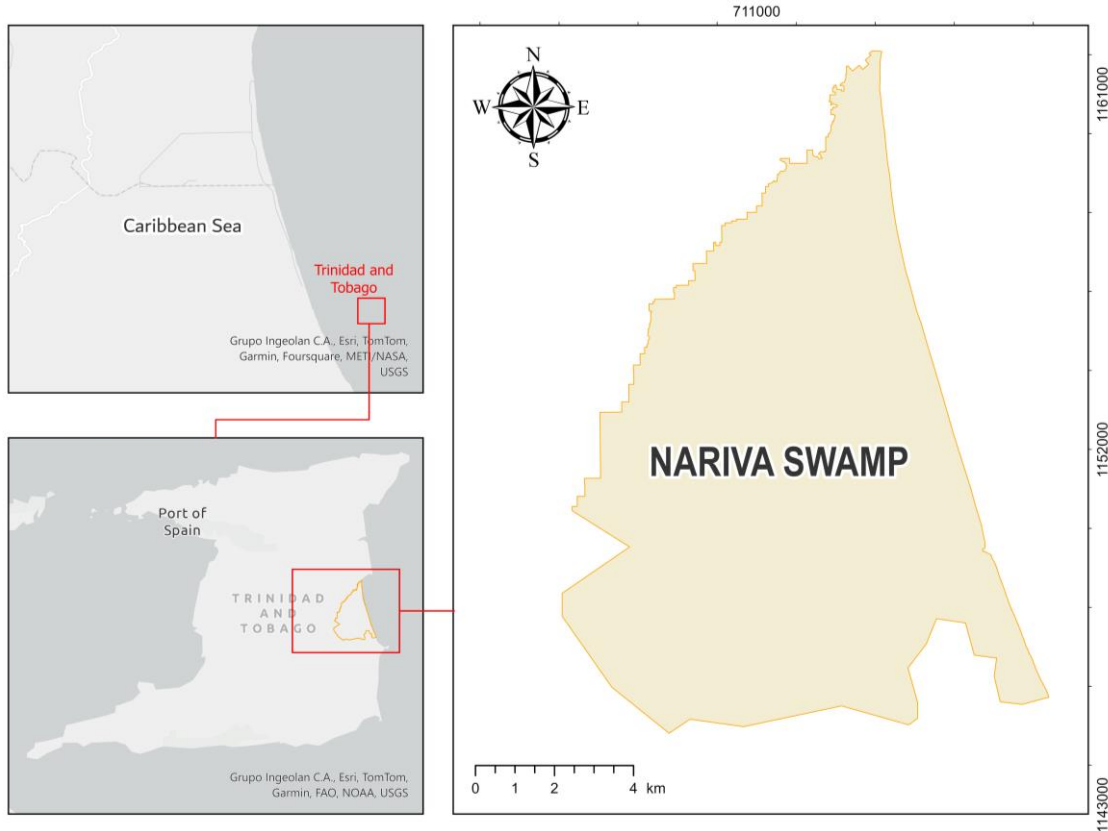


Figure 1. Study area location in Nariva Swamp, Trinidad and Tobago

imagery has also been used more frequently in recent years (Acharki, 2022; Vizzari, 2022). While all three satellites capture images with fairly high spectral resolution, they vary regarding their respective spatial resolutions. Landsat-8 imagery is often considered low spatial resolution with a 30 m per pixel resolution for its main bands while Sentinel imagery is considered medium spatial resolution with a 10 m per pixel resolution for its key bands (Loukika et al., 2021). PlanetScope imagery provides a higher spatial resolution with 3–5 m per pixel, and is more widely utilized for smaller study areas (Acharki, 2022; Basheer et al., 2022). Studies have also demonstrated that as spatial and spectral resolution increase, classification accuracy typically increases (Acharki, 2022). For this study, PlanetScope SuperDove (PSB.SD) 3 m per pixel satellite imagery was utilized since the area of study as well as some of the individual classes were small. As a result, it was determined that any classification to be conducted would greatly benefit from the higher spatial resolution of this imagery.

The main goal of this study was to develop an updated LULC map of the Nariva Swamp region using a machine learning approach and PlanetScope SuperDove (PSB.SD) 3 m per pixel

satellite imagery. The following objectives were implemented in order to achieve this goal, three different machine learning (ML) algorithms were applied and the output maps generated were evaluated to determine which one was best suited for developing LULC maps for the Nariva Swamp, a final 2024 LULC map of the Nariva Swamp was then produced by applying the best performing ML algorithm and finally, a land cover change assessment was conducted by comparing the 2024 LULC map produced to a previously developed 2009 LULC map.

2. MATERIALS AND METHODS

2.1 Study Area

The Nariva Swamp (Figure 1), one of several wetlands in Trinidad and Tobago, is found along the eastern coast of Trinidad at 10°23' N and 061°04' W (Darsan et al., 2013; Stewart et al., 2022). It spans approximately 113.4 km² and serves as a catchment area for the Nariva River, discharging into the southern end of its eastern border at the Cocal, a sand bar known as Manzanilla beach, which separates it from the Atlantic Ocean (Darsan et al., 2013; Stewart et al., 2022). Despite Trinidad's relatively small size and tropical climate, there are

notable variations in the yearly average precipitation levels (Dookie et al., 2018). The eastern region of Central Trinidad, known as the wet belt, receives substantial rainfall of approximately 90–120 inches (2286–3048 mm) annually. On the other hand, the southern part of Trinidad is characterized by a drier climate, with an average annual rainfall below 80 inches (2032 mm) except for a narrow strip on the east coast and the northern flanks of the Southern Range (Roopnarine et al., 2022).

The Nariva Swamp is not only the largest wetland but also the largest freshwater swamp system in Trinidad and Tobago (Juman & Hassanali, 2013). The region showcases a rich tapestry of natural elements, encompassing coastal beaches, freshwater marshes, palm swamps, freshwater swamp woods, and mangroves (Baptiste & Smardon, 2012). This intricate blend of habitats provides a nurturing environment for a wide array of wildlife, boasting an impressive diversity of flora and fauna inclusive of 176 species of birds, 45 species of mammals, 39 species of reptiles, 19 species of frogs, 33 species of fish, 28 species of spiders, 15 species of snails and conch, 213 species of insects, and an impressive count of over 319 plant species (FAO, 2019).

The Nariva Swamp is surrounded by several local communities, Plum Mitan, situated to the North, Biche located to the West, and Kernahan, positioned on the South-East (Carbonell & Nathai-Gyan, 2005). The swamp has been utilized by these communities for small-scale subsistence farming, fishing, hunting and housing development since the 1930s (FAO, 2019).

The increasing demand for staple food items prompted the implementation of an exclusionary zone for rice farming in the 1950s, known as Rice Project A or Plum Mitan Rice Scheme (FAO, 2019). This agricultural endeavor led to the clearance of an estimated 5 km² of wetland and forest to construct drainage and irrigation channels, dividing the land into agricultural plots (FAO, 2019). Another developmental project, the Navet Dam, constructed in the 1960s to supply growing residential areas in the west, reduced the water volume reaching the Nariva system (FAO, 2019). In the 1980s, large-scale commercial farmers from other parts of the country arrived to exploit the wet rice paddy prospects in the area (FAO, 2019). They cleared and prepared 15 km² of land south of the Plum Mitan Rice Scheme, known as Rice Project B, using agrochemicals, heavy machinery, and fires (FAO, 2019). In response to their harmful farming practices, environmentalists and the media campaigned for their removal, resulting in their

expulsion in 1996 after the 'Battle of Nariva' from 1993 to 1996 (Carbonell & Nathai-Gyan, 2005; FAO, 2019).

Apart from these human activities impacting the Nariva system, environmental threats include saltwater intrusion, coastal erosion, and rising sea levels (Darsan et al., 2013; Juman & Ramsewak, 2013). Although numerous institutions have expressed interest in exploring oil reserves in the area, they have been unable to obtain permission to do so within the protected confines of the swamp (Jaggernaut, 2012). As a result, they have drilled as close as possible without crossing the boundary (Jaggernaut, 2012).

Over the years, the management of the Nariva Swamp has undergone various changes and initiatives. It was initially protected by the Forestry and Wildlife legislation and was later declared a Wetland of Ecological Importance under the Ramsar Convention in 1993 (Juman & Hassanali, 2013). Subsequently, the Government of the Republic of Trinidad and Tobago included the Nariva Swamp in the Montreaux Record and requested a Ramsar Advisory Mission, leading to recommendations aimed at enhancing wetland management (Juman & Hassanali, 2013). These suggestions included conducting an environmental impact assessment, implementing a management plan, and developing a restorative plan focused on hydrology, aquatic vegetation, and firefighting (Juman & Hassanali, 2013). In 2006, the swamp was designated an Environmentally Sensitive Area under the Environmental Management Act, fostering collaboration between community-based organizations, the University of the West Indies, and the Forestry Division (Juman & Hassanali, 2013). This collaboration resulted in the establishment of the Nariva Swamp Restoration, Carbon Sequestration, and Livelihoods Project in 2011 (Juman & Hassanali, 2013).

2.2 Data Sources

High-resolution PSB.SD 3 m per pixel satellite imagery was accessed from the Planet Labs database. This imagery was selected as it presents a high spatial and spectral resolution compared to other publicly available satellite imagery commonly used (Table 1) (Kpienbaareh et al., 2021; Aldiansyah & Saputra, 2022). Imagery for January 24, 2024, was selected to be used for the final classified map as this imagery contained the lowest cloud cover and required the least preprocessing. Additional images for the months of January and February of 2023 as well as images from January and February of 2024 were also

Table 1. Comparison of publicly available satellite imagery

| Imagery Data Layer | Sources | Bands | Central Wavelength (µm) | Spatial Resolution (m) |
|---|---------------------------|-------|-------------------------|------------------------|
| PlanetScope SuperDove (PSB.SD) 3m per pixel satellite imagery | PlanetScope | 8 | 0.443-0.865 | 3 |
| Landsat-8 Operational Land Imager surface reflectance Tier 1 | Google Earth Engine (GEE) | 11 | 0.04-12.51 | 30 |
| Sentinel-2 MSI: Multispectral Instrument, Level-1C | Google Earth Engine (GEE) | 13 | 0.44-2.2 | 10-20 |

obtained which were used to assist with training as well cloud masking. A combination of the Google Earth Engine (GEE) platform and ESRI's ArcGIS Pro software was used to carry out the preprocessing of the imagery in order to perform cloud masking and extraction of the study area. For the classification of the imagery, all 8 bands of the PlanetScope data were used. **Figure 2** depicts a sample of a PSB.SD 3 m per pixel satellite image used in this study.



Figure 2. Example of a PSB.SD 3 m per pixel satellite imagery mosaic used in the study

The classification scheme used in this study comprised of eight classes as follows: coconut; forest; agriculture; mangrove; non-forested wetland; sandy beach; urban development and water and was adapted from a previous study (FAO, 2019) as well as preliminary in-situ surveys of the study area.

For the study, 485 field sample points were collected across the eight identified land cover classes (Table 2) to be used for training and accuracy assessment of the ML algorithms. GEE was used to train and execute all three algorithms used in the study, adapting a similar methodology to one used for the development of a LULC for Munneru river basin in India (Loukika et al., 2021). The platform's built-in functions for the classifiers provided the basis for the algorithms used:

Support vector machine (SVM) algorithm via the "Classifier.libsvm" method which operates by creating an optimal hyperplane during training to separate classes with minimal misclassification (Basheer et al., 2022).

Classification and regression tree (CART) algorithm via the "Classifier.smileCart" method which operates by recursively partitioning data based on a chosen threshold until reaching terminal nodes. The data is divided into groups, generating trees using subsets of these groups (Basheer et al., 2022).

Random forest (RF) algorithm via the "Classifier.smileRandomForest" method which operates by mixing multiple CART models to construct decision trees by randomly selecting training datasets and features (Basheer et al., 2022).

2.8 Methodology

A key aspect of this study involved obtaining field data which could be used to train the ML algorithms as well as to assess the accuracy of the developed LULC maps. Data was collected within two sections of the Nariva Swamp as well as along the eastern boundaries (Figure 3). A total of 485 field GPS coordinates were collected over a two-day period in February 2024. The collected coordinates were split into training and accuracy assessment datasets in a ratio of approximately 70:30 as this ratio has been shown to produce a high level of accuracy (Odindi et al., 2014; Aldiansyah & Saputra, 2022).

Table 2. Number of field sample points collected for each land cover class in the classification scheme used

| Land Cover Classes | Number of Sample Points |
|----------------------|-------------------------|
| Water | 50 |
| Coconut | 49 |
| Agriculture | 163 |
| Non-forested Wetland | 40 |
| Mangrove | 59 |
| Forest | 71 |
| Sandy Beach | 15 |
| Urban Development | 38 |

Following this, the cloud rectified image was imported into GEE along with supplementary raster data of the Nariva Swamp and the set of 317 training sample points collected during the ground truthing exercise. Additional points were generated using information from high resolution Google maps imagery (Vizzari, 2022), additionally obtained satellite imagery and observational data collected during the ground truthing exercise in order to ensure a minimum of 50 training points were provided for each class in the classification scheme (Lillesand et al., 2015).

Figure 4 illustrates the methodological workflow implemented for classifying the imagery using the selected ML algorithms and comparison of the outputs to determine the most accurate/suitable product. The imagery selected as the primary input for the classification was first imported into ArcGIS Pro along with supporting imagery in order to remove cloud shadow and cloud cover (Liedtke & Simon, 2022).

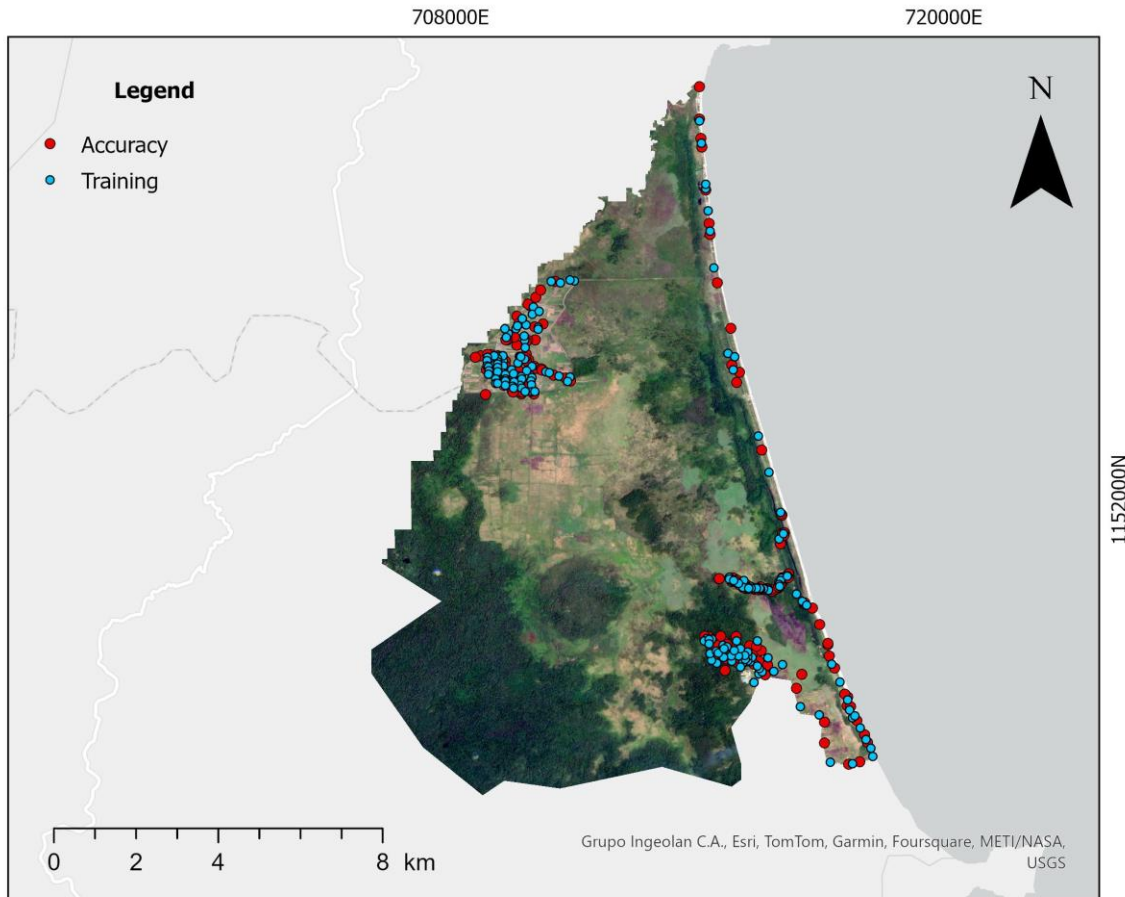


Figure 3. Study data collection locations within the Nariva Swamp.

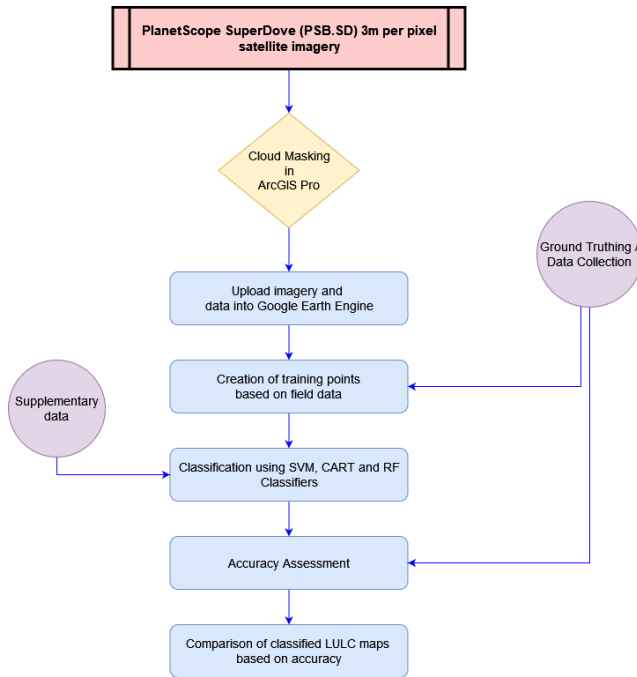


Figure 4. Methodology used for the LULC classification of PSB.SD 3 m per pixel satellite imagery

Table 3 Name and description of the LULC classification scheme used in the study

| Class Name | Description of Class |
|----------------------|---|
| Coconut | Areas dominated by coconut palm trees greater than 20% of total vegetative cover. |
| Forest | Areas dominated by trees generally greater than 5 meters tall and greater than 20% of total vegetation cover. |
| Water | Areas of open water, generally with less than 25% cover vegetation or soil. |
| Agriculture | Areas used for the production of annual, perennial or other types of crops. Crop vegetation accounts for greater than 20% of the total vegetation |
| Mangrove | Areas dominated by mangrove cover and comprise more than 20% of total vegetation. |
| Non-forested Wetland | Areas where perennial herbaceous vegetation accounts for greater than 80% of vegetative cover and the soil or substrate is periodically saturated with or covered with water. |
| Urban Development | Areas with a mixture of constructed materials and vegetation. Impervious surfaces account for 20 to 79% of the total cover. |
| Sandy Beach | Coastal land comprising of sandy substrate. Generally, vegetation accounts for less than 15% of total cover. |

The classification scheme used in this study was based on a scheme created in 2009 (FAO, 2019). The original scheme contained a total of 14 classes, however based on preliminary studies of the area it was determined that several of the classes either no longer existed or could be grouped into a single class due to their similar function and spectral reflectance. It is assumed that the reduction in the number of

classes also served to further increase the accuracy of the final classified map as studies have suggested that map accuracy may decrease as the number of classes increase (Thin et al., 2019). Using the original scheme and additional guidance provided by the Anderson Land Cover Classification System (Anderson et al., 1976), the resulting scheme used for this study was comprised of eight identified classes which are listed in Table 3: coconut; forest (which combined the forest, forested wetland and mixed forest); water; agriculture (which encompasses active and fallow crops); mangrove; non-forested wetland (which combined non-forested wetland, freshwater marsh dieback, grasslands as well as former rice areas in succession); urban development (which combined urban residential and urban transport); and sandy beach.

For the random forest classifier, a value of 100 was selected for the number of trees as this provided the highest accuracy and performance while for the CART classifier, the optimum cross-validation factor was set at 10 based on previous studies (Kohavi, 1995). The SVM classifier required several inputs to produce accurate results. For the classification, it was found that the C-SVC type worked best with a linear kernel type and a cost (C) value of five.

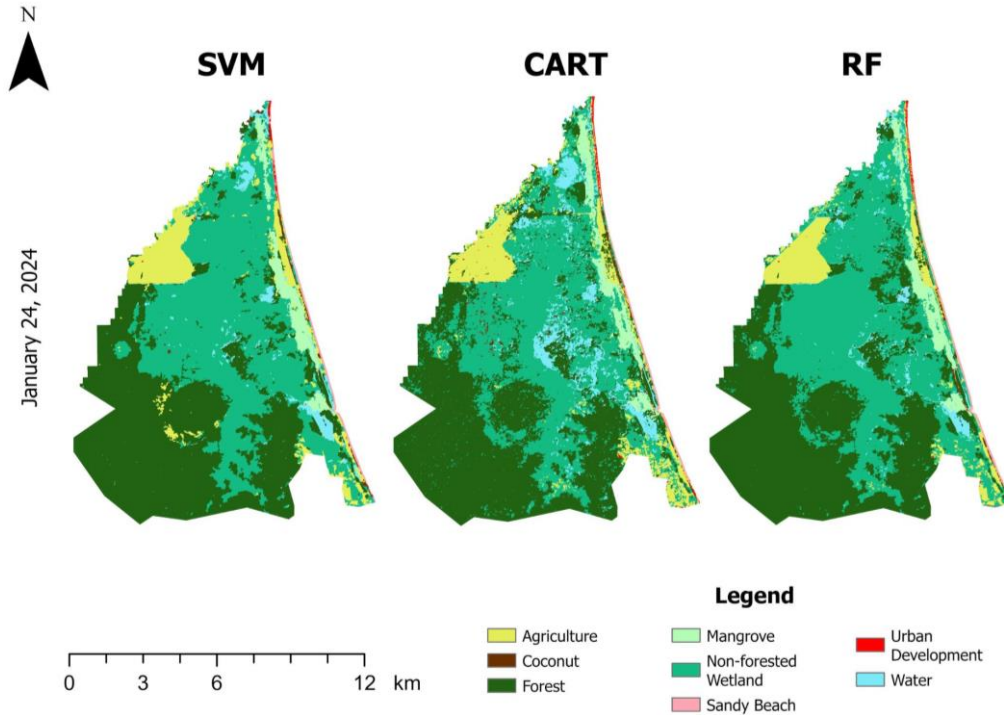


Figure 5. Classified LULC maps of the Nariva Swamp created using PSB.SD 3m per pixel satellite imagery and SVM, CART, and RF classifiers in GEE for January 24, 2024

The accuracy of each model was determined using a confusion matrix which determined the overall accuracy for the maps produced using each method, as well as their respective producer's and user's accuracy. A kappa coefficient was also calculated for each produced map for comparison. These metrics are frequently used throughout similar studies (Nandy et al., 2017; Loukika et al., 2021; Basheer et al., 2022; Vizzari, 2022) as a means of comparing the performance of different classifiers. The accuracy assessment dataset, which consisted of 168 data points, was utilized for the error matrix. To perform the accuracy assessment, the data sample points selected for accuracy assessment were overlain onto each of the produced maps within GEE. The overall accuracy of each map was calculated using the following equation:

$$\text{Overall Accuracy (OA)} = T_c / T_s \times 100 \quad (1)$$

Where T_c represents the total number of correctly classified pixels and T_s represents the total number of sample pixels. The kappa coefficients were calculated using the equation:

$$\text{kappa coefficient (k)} = (OA - CA) / (1 - CA) \quad (2)$$

Where OA is the overall accuracy and CA the chance of agreement. The PA was calculated by dividing the total number of classified points that agree with the reference data by the total number of sample pixels used that class, while the UA was calculated by dividing the total number of classified pixels that agree with the reference data by the total number of classified pixels for that class.

The map with the highest OA was selected as the final output map and then used to carry out a change detection analysis against the LULC map produced in 2009. Several methods have been used for change detection of LULC using different sources of satellite imagery (Lu et al., 2004) however, the method used in this study is based on the comparison of recent LULC data against the classified map produced in 2009. In order to carry out the change detection analysis, changes in areal coverage between the 2024 LULC map classified map produced using the ML classifier were compared against those of the previously developed 2009 LULC map. For classes that were combined in the updated 2024 classification scheme used in this study, the area of each class merged from the 2009 LULC map were summed up and compared.

3. RESULTS

3.1 ML LULC Classification Maps

Figure 5 illustrates the preliminary LULC maps produced using the ML CART, SVM and RF classifiers. From the results, all three classifiers indicated that the largest land cover class was non-forested wetland followed by the forest class. The results produced by all three classifiers also identified the presence of agriculture in the northwestern and southeastern sections of the study

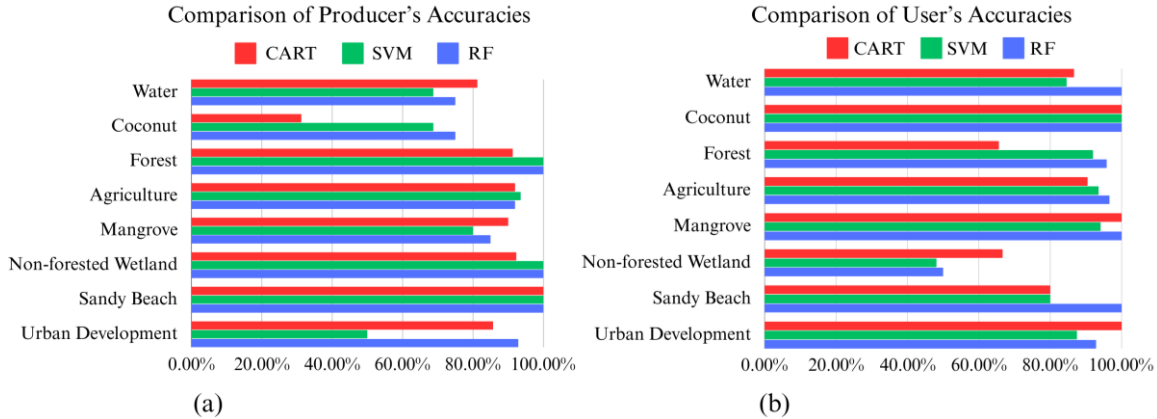


Figure 6. Comparison of producer's (a) and user's (b) accuracies of the CART, SVM and RF classifiers

Table 4 Overall Accuracy and kappa coefficient of maps produced using CART, SVM and RF Classifiers

| Classifier | Overall Accuracy (OA) | Kappa Coefficient (k) |
|------------|-----------------------|-----------------------|
| CART | 85% | 0.886 |
| SVM | 85% | 0.893 |
| RF | 90% | 0.934 |

area. The map produced using the CART classifier displayed larger water and mangrove classes than the other two classifiers. Both the CART and SVM classifiers generally had challenges with the classification of the coconut class, with the CART classifier resulting in much of the coconut class being misclassified as agriculture. The CART classifier also indicated the presence of small sections of coconut within the central areas of the Nariva Swamp which was also seen on a smaller scale in the map produced using the SVM classifier.

The map produced using the CART classifier appeared a lot more scattered than the other maps produced, resulting in pixels of forest and non-forested wetland classes scattered throughout the map. The results also indicated that the SVM classifier misclassified sections of water as non-forested wetland, agriculture and mangrove and of the three classifiers SVM had the most difficulty with the detection of the water class. This classifier also misclassified significant amounts of urban development as non-forested wetlands.

While all three classifiers demonstrated some difficulty with the classification of the water class, the CART classifier performed better than the SVM and the RF. CART also outperformed both

other classifiers when detecting mangroves. All three classifiers performed exceptionally well with the classification of the forest and sandy beach classes.

The overall results of the comparative assessment showed that the RF classifier outperformed both the SVM and CART classifiers.

3.2 Accuracy Assessment

From the data collected in the field, an independent subset of GPS points was selected specifically for accuracy assessment of the produced maps and was not used in the training of the algorithms. **Table 4** depicts the results of the accuracy assessment for all three classifiers while **Figure 6** presents a comparison of the PA and UA for the maps created using each of the three classifiers. The results of the confusion matrix determined that the overall accuracy (OA) of the maps produced using the SVM and CART classifiers were both 85% while the OA of the map produced with the RF classifier was 90%. The kappa coefficients calculated for the classified maps were found to be 0.886, 0.893 and 0.934 for the CART, SVM and RF classifiers respectively. The producer's accuracy (PA) for the map produced with the CART classifier was highest for the sandy beach class at 100%. The CART classifier also resulted in a PA of 90% and above in four of the other classes: 92.31% for non-forested wetlands; 91.94% for agriculture; 91.30% for forest; and 90% for mangrove. Both the water and urban development classes had PA over 80% with urban development resulting in 85.71% producer's accuracy and water, 81.25%. This classifier, however, demonstrated difficulty with the coconut class and resulted in a PA of 31.25% in this class.

The SVM classified map demonstrated high PA for four of the classes: 100% for sandy beach, non-forested wetland and forest; and 93.55% for

agriculture. The mangrove class also resulted in a good PA with 80%. This classifier struggled however, with the water, coconut and urban development classes with PA values of 68.75% for water and coconut; and 50% for urban development.

The map created using the RF classifier demonstrated PA values of over 90% for five of the eight classes with forest, non-forested wetland and sandy beach all resulting in 100%. The agriculture class resulted in a PA of 91.94% and the urban development class resulted in a PA of 92.86%. The RF classifier demonstrated some level of difficulty with the coconut and water classes resulting in a PA of 75% for both classes.

The UA varied for all three classifiers across all eight classes. The results of the map created using the CART classifier indicated that the UA for four of the classes exceeded 90%. The UA for urban development, coconut and mangrove were all 100% while the agriculture class had a UA of 90.48%. The water and sandy beach classes also resulted in good UA values with the water and sandy beach classes having UA values of 86.67% and 80% respectively. The forest and non-forested wetland classes had the lowest UA with 65.63% and 66.67% respectively.

UA calculated for the SVM classified map ranged from 48.15% for non-forested wetland to 100% for coconut. The forest, agriculture and mangrove classes had UA of 92%, 93.55% and 94.12% while the water, sandy beach and urban development classes resulted in UA of 84.62%, 80% and 87.5% respectively.

The map generated using the RF classifier had UA values of over 90% for seven of the eight classes. The water, coconut, mangrove and sandy beach classes all had accuracies of 100% while forest, agriculture and urban development had accuracies of 95.83%, 96.61% and 92.86% respectively. The lowest UA for this map was seen with the non-forested wetland class which had a result of 50%.

The results of the confusion matrix indicated that among the three classifiers, the RF classifier produced the map with the highest OA and kappa coefficient. The RF classified map also demonstrated consistently high producer's and user's accuracies across most classes. Based on this, the RF classified map was selected as the final 2024 classified LULC output map and was used in conjunction with the 2009 LULC map to conduct the change detection analysis.

3.2 LULC Change Detection

The LULC change detection method used in this study required that the classes in both the 2024 RF classified LULC map and the 2009 classified LULC map be homogenized for a more equitable comparison. **Figure 7** presents a visual comparison of the homogenized 2009 classified map (FAO, 2019) and the 2024 RF classified map. From a visual comparison several similarities can be observed. The distribution of the different land cover types across the study area has remained more or less unchanged, however, the distribution of the coconut class is notably reduced in the 2024 map. The 2024 map also displays a larger mangrove class as compared to the 2009 LULC map indicating that the mangrove forest coverage has expanded.

Further analysis of the total areal coverage of each land cover class revealed the extent of the changes to some of the classes within the Nariva Swamp. **Table 5** provides a summary of the areas (in km²) of each land type for both the 2009 LULC map and the 2024 LULC map. From the results it can be seen that over the 15-year period there has been a decrease in the coconut, forest, agriculture and sandy beach classes, while there has been an increase in the water, mangrove, non-forested wetland and urban development classes.

The most notable changes observed based on LULC areal coverage were for the forest and non-forested wetland classes. Based on the analysis, forest cover decreased by 3.84 km² within the Nariva Swamp while the non-forested wetland increased by 3.31 km². The results for percentage area change indicated that the water cover within the study area increased by 255.87%. Areas classified as urban development were also observed to have increased by 116.67%. Coconut coverage was observed to have decreased by 80.47% while sandy beach decreased by 25.26%.

4. DISCUSSION

This study utilized PlanetScope SuperDove (PSB.SD) 3 m per pixel satellite imagery and different machine learning (ML) algorithms to develop a 2024 LULC map of the Nariva Swamp with a 90% overall accuracy. The use of PlanetScope SuperDove (PSB.SD) 3 m per pixel satellite imagery was a key contributing factor in this outcome as the small study area size benefitted from the high spectral and spatial resolution imagery in order to better classify smaller target

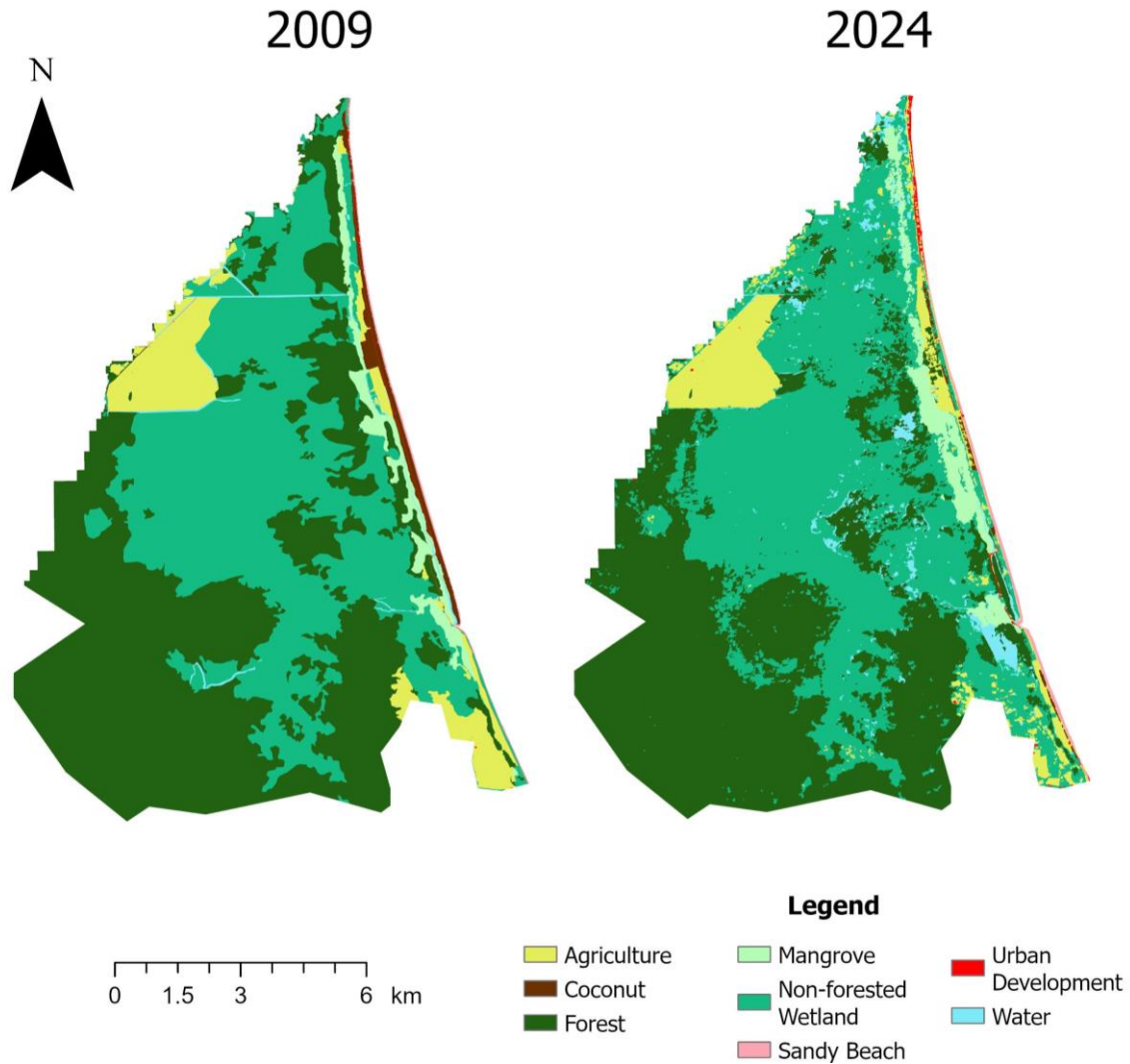


Figure 7 Classified LULC maps of the Nariva Swamp, 2009 and 2024

Table 5 Change in the area or each land cover class from 2009 to 2024

| Land use/cover Classes in 2024 RF classified map | Area (km ²) | Land use/cover in 2009 classified map | Area (km ²) | Difference (km ²) | Difference (%) |
|--|-------------------------|---------------------------------------|-------------------------|-------------------------------|----------------|
| Water | 2.73 | Water | 0.766 | 1.96 | 255.87 |
| Urban Development | 0.39 | *Urban Development | 0.18 | 0.21 | 116.67 |
| Mangrove | 3.54 | Mangrove | 3.01 | 0.53 | 17.61 |
| Non-forested Wetland | 49.27 | **Non-forested Wetland | 45.96 | 3.31 | 7.2 |
| Coconut | 0.33 | Coconut | 1.69 | -1.36 | -80.47 |
| Sandy Beach | 0.71 | Sandy Beach | 0.95 | -0.24 | -25.26 |
| Agriculture | 7.33 | ***Agriculture | 7.96 | -0.63 | -7.91 |
| Forest | 49.1 | ****Forest | 52.94 | -3.84 | -7.25 |

* Encompasses urban residential and urban transport classes from the 2009 classified map

** Encompasses non-forested wetland, freshwater marsh dieback, grasslands and former rice areas in succession classes from the 2009 classified map

*** Encompasses active and fallow crops classes from the 2009 classified map

**** Encompasses the forest, forested wetland and mixed forest classes from the 2009 classified map

classes. Similar findings were also discussed in previous studies which compared the accuracy of classified maps using satellite imagery of different spatial resolutions (Basheer et al., 2022; Vizzari, 2022). A review of previous studies which utilized satellite imagery of lower spatial resolution, such as Landsat-8 or Sentinel-2 satellite, demonstrated that the overall accuracy of classified maps using these data sources were generally high for larger study areas but did not perform as well in smaller study areas (Wang et al., 2019; Loukika et al., 2021; Aldiansyah & Saputra, 2022; Basheer et al., 2022; Vizzari, 2022).

The ML algorithms used in this methodology were based on their performance in previous studies. Several studies have shown that the CART, SVM and RF ML algorithms tend to be highly reliable at producing high accuracy LULC maps of OA above 80% (Wang et al., 2019; Loukika et al., 2021; Aldiansyah & Saputra, 2022; Basheer et al., 2022; Vizzari, 2022). This was further reflected in the results obtained in this study with all three classifiers producing maps with OA above 80%. Further, the results of this study demonstrated that the RF classifier produced the best results with an OA of 90%. This was also seen in other studies which also compared the performance of ML classifiers in other wetland ecosystems (Wang et al., 2019). Generally, the RF classifier has been demonstrated to perform best with classification of largely vegetated areas and is able to handle a larger number of features and a smaller number of samples than both the CART and SVM classifiers (Wang et al., 2019). The SVM classifiers have been shown to perform better in areas with higher urban development (Basheer et al., 2022) and may be more suited for use in those environments. CART classifiers have also been shown to perform well in several situations (Basheer et al., 2022), however, these classifiers may be prone to overfitting which can reduce their accuracy (Qian et al., 2014). This was demonstrated in the results of this study as the overfitting of data from the CART classifier likely resulted in the lower PA and higher UA seen for several LULC classes.

From the results of the study, it was seen that all three classifiers displayed varying levels of difficulty with classifying the coconut class. This could have been due to the more scattered distribution of the coconut land cover which was observed during the field data collection. Several areas of coconut were observed interspersed amongst other LULC classes such as agriculture and non-forested wetland which could have resulted in some levels of misclassification. Comparable challenges were also noted in previous studies (Pham et al., 2022) which would have examined similar LULC classes along coastal areas. Comparison with the LULC map developed in 2009 revealed that the percentage decrease in coconut

coverage was quite significant in the 2024 LULC map, and the smaller land cover area would have also increased the risk of misclassification by the algorithms. The 2009 LULC map was developed using a combination of traditional approaches, including visual interpretation and unsupervised classification of Landsat satellite imagery. While these methods and data were widely used at the time and produced a good understanding of land cover changes, they were limited by the lower spatial and spectral resolution of the imagery as well as the subjective nature of the visual interpretation procedure (Rozenstein & Karnieli, 2011). In contrast, the approach used to develop the 2024 LULC map offered significant advantages, including higher spatial and spectral resolutions, which allowed for more precise delineation of smaller land cover features and reduced risk of misclassification (Vizzari, 2022). However, the RF approach also has its limitations compared to the 2009 approach, particularly its reliance on high-quality training data (Mashala et al., 2023).

The change analysis performed as part of this study was essential to understanding how the LULC of the Nariva Swamp has changed over time. The results indicated that there was a significant increase in the non-forested wetland and a decrease in forest. This may suggest an expansion of the non-forested wetlands within the Nariva Swamp at the expense of forest. Similar findings were also noted in another study in India which noted a decrease in forest cover and an increase in non-forest cover (Thakur et al., 2024). Other notable changes included an increase in both water and urban coverage. The increased water coverage could have been as a result of misclassification as the performance of the RF classifier was low when detecting water areas. Other factors may also be responsible for the calculated increase in water class which may include climate change and sea level rise (Cahoon et al., 2019) leading to an actual increase in water coverage in the region. The changes to urban development may also be of concern as this may be an indicator of unregulated development within the Nariva Swamp.

While the findings of the study offer valuable insight into the use of ML and RF for the creation of LULC maps of the Nariva Swamp, it is important to acknowledge several limitations and potential improvements that could be made regarding the study. Obtaining field data sample points proved to be especially challenging. Access to the study site on foot was limited to specific sections of the southeastern and northwestern parts of the swamp and along the eastern boundary. This introduced a level of accessibility bias into the study and resulted in some difficulty with obtaining points representative of other areas within the Nariva Swamp. To compensate for this to some extent,

further sample points were generated from high resolution Google Maps imagery in conjunction with observations that were made while conducting the ground truthing exercise and additional satellite imagery. This method has also been used in other studies to achieve a similar result (Vizzari, 2022). The use of drones can be one potential strategy for obtaining such challenging data for future studies. The requisite logistics and approvals associated with the use of this technology must be implemented in advance for this to be an effective solution.

5. CONCLUSION

The findings of this study offer a simple and efficient approach for generating updated LULC maps for the Nariva Swamp which can be adapted to other similar environments particularly within the Caribbean region. The RF classifier was seen to be the superior of the three classifiers used for the study, having produced a map of a higher overall accuracy and kappa coefficient. This research also provides a reliable method for monitoring LULC changes within the Nariva Swamp. The comparison between the 2024 LULC developed map and the 2009 LULC existing map revealed increases in water, urban, mangrove and non-forested wetland coverage in the Nariva Swamp between 2009 and 2024. It was also revealed that there was a decrease in forest cover over the 15-year period. The updated 2024 LULC map developed as a result of this study as well as the methodological approach implemented can be used for monitoring changes in

the Nariva Swamp moving forward. The overall output can serve as an invaluable tool for enhancing environmental management strategies, facilitating informed decision-making, and ultimately fostering the sustainable conservation of the wetland ecosystems in the Nariva Swamp. Furthermore, factors such as climate change and sea-level rise, population growth and socioeconomic variables must be considered in future studies and planning.

Author Contributions. Deanesh Ramsewak: Conceptualization, Methodology, Data Curation, Formal analysis, Writing – review and editing, Visualization. Mickell Gunnesslal: Conceptualization, Methodology, Data Curation, Formal analysis, Writing – review & editing, Visualization. Arvind Jagassar: Methodology, Writing – review & editing, Visualization. Arthur Potts: Supervision, Writing – review & editing, Visualization.

Acknowledgments. The authors would like to express their gratitude to the Environmental Management Authority (EMA) of The Ministry of Planning and Development and The Forestry Division of the Ministry of Agriculture, Land and Fisheries of Trinidad and Tobago for their support throughout this study. We would also like to thank Mr. Tevin Butler, Mr. Rainer Deo and Mr. Jason Edwards for their support in the field data collection aspect of this study. Finally, we would like to thank the anonymous reviewers for taking the time to provide valuable feedback towards the improvement of this article.

Funding. This research did not receive any specific grant from funding agencies in the public, commercial, or not-for-profit sectors.

REFERENCES

- Acharki, S. 2022. PlanetScope contributions compared to Sentinel-2, and Landsat-8 for LULC mapping. *Remote Sensing Applications: Society and Environment*, **27**, 22 pp. doi:10.1016/j.rsase.2022.100774
- Aldiansyah, S. and Saputra, R.A. 2022. Comparison of machine learning algorithms for land use and land cover analysis using Google Earth Engine (case study: Wanggu Watershed). *International Journal of Remote Sensing and Earth Sciences*, **19**(2), 197–210.
- Anderson, J.R., Hardy, E.E., Roach, J.T. and Witmer, R.E. 1976. A land use and land cover classification system for use with remote sensor data. pp. iii–28. doi: 10.3133/pp964
- Baptiste, K.A. and Smardon, C.R. 2012. A review of wetland use and management of the Nariva Swamp, Trinidad. *Caribbean Geography*, **17**(1), 73–91.
- Basheer, S., Wang, X., Farooque, A.A., Nawaz, R.A., Liu, K., Adekanmbi, T. and Liu, S. 2022. Comparison of land use land cover classifiers using different satellite imagery and machine learning techniques. *Remote Sensing*, **14**(19), 18 pp. doi: 10.3390/rs14194978
- Cahoon, D.R., Lynch, J.C., Roman, C.T., Schmit, J.P. and Skidds, D.E. 2019. Evaluating the relationship among wetland vertical development, elevation capital, sea-level rise, and tidal marsh sustainability. *Estuaries and Coasts*, **42**(1), 1–15. doi: 10.1007/s12237-018-0448-x
- Carbonell, M. and Nathai-Gyan, N. 2005. Nariva Swamp Ramsar Site, Trinidad and Tobago (West Indies) Wetland Habitat Restoration Initiative. USDA Forest Service General Technical Report, 191, pp. 446–449.
- Cecili, G., De Fioravante, P., Dichicco, P., Congedo, L., Marchetti, M. and Munafò, M. 2023. Land cover mapping with convolutional neural networks using Sentinel-2 images: case study of Rome. *Land*, **12**(4), 20 pp. doi: 10.3390/land12040879
- Choi, C.Y., Xiao, H., Jia, M., Jackson, M.V., Lai, Y.C., Murray, N.J., Gibson, L. and Fuller, R.A. 2022. An emerging coastal wetland management dilemma between mangrove expansion and shorebird conservation. *Conservation Biology*, **36**(5), 11 pp. doi: 10.1111/cobi.13905
- Darsan, J., Asmath, H. and Jehu, A. 2013. Flood-risk

- mapping for storm surge and tsunami at Cocos Bay (Manzanilla), Trinidad. *Journal of Coastal Conservation*, **17**(3). 679–689. doi: 10.1007/s11852-013-0276-x
- Dookie, N., Chadee, T.X. and Clarke, R.M. 2018.** Trends in extreme temperature and precipitation indices for the Caribbean small islands: Trinidad and Tobago. *Theoretical and Applied Climatology*, **136**(1–2), 31–44. <https://doi.org/10.1007/s00704-018-2463-z>
- Digra, M., Dhir, R. and Sharma, N. 2022.** Land use land cover classification of remote sensing images based on the deep learning approaches: a statistical analysis and review. *Arabian Journal of Geosciences*, **15**(10), 1003, 24 pp. doi: 10.1007/s12517-022-10246-8
- Food and Agriculture Organization. 2019.** *Management plan for the Nariva Swamp Protected Area*. Technical Report, Institute of Marine Affairs, 09, 93 pp.
- Jaggernauth, D.J. 2012.** The challenges facing independent companies willing to extract crude oil on the periphery of the Nariva Swamp, an environmental sensitive area in Trinidad. *All Days. SPE Annual Technical Conference and Exhibition*, 11 pp. doi: 10.2118/157609-MS
- Jalim, R. 2015.** UNDP: Sinking into paradise - Climate change worsening coastal erosion in Trinidad. <https://www.preventionweb.net/news/undp-sinking-paradise-climate-change-worsening-coastal-erosion-trinidad>
- Juman, R.A. and Ramsewak, D. 2013.** Status of Mangrove Forests in Trinidad and Tobago, West Indies. *Caribbean Journal of Science*, **47**(2–3), 291–304.
- Juman R.A. and Hassanali K. 2013.** Mangrove Conservation in Trinidad and Tobago, West Indies. *Mangrove Ecosystems: Biogeography, Genetic Diversity and Conservation Strategies*. Mangrove Ecosystems. *Environmental Research Advances*, **1**(2), 35–63
- Kohavi, R. 1995.** A Study of Cross-Validation and Bootstrap for Accuracy Estimation and Model Selection. *International Joint Conference on Artificial Intelligence*, **14**(2), 1137–1145
- Kpienbaareh, D., Sun, X., Wang, J., Luginaah, I., Kerr, R.B., Lupafya, E. and Dakishoni, L. 2021.** Crop type and land cover mapping in northern Malawi using the integration of sentinel-1, sentinel-2, and planetscope satellite data. *Remote Sensing*, **13**(4), 1–21. doi: 10.3390/rs13040700
- Lagomasino, D., Fatoyinbo, T., Payton, A., Taillie, P. J., Goldberg, L., Montesano, P., Neigh, C.S.R., Corp, L.A., Cook, B., Morton, D.C. and Roman-Cuesta, R.M. 2019.** Hurricane-related forest degradation and dieback across the Caribbean. *AGU Fall Meeting Abstracts*, 2019, p. GC43A-11.
- Liedtke, J. and Simon, W. 2022.** “The Cloud Eradicator.” *ArcGIS Blog, Esri. May 3, 2022.* <https://www.esri.com/arcgis-blog/products/arcgis-pro/imagery/the-cloud-eradicator/>
- Lillesand, T.M., Kiefer, W.R and Chipman, W.J. 2015.** *Remote Sensing and Image Interpretation*, 7th ed. Hoboken, NJ: John Wiley & Sons, Inc., 768 pp., Google Books.
- Loukika, K.N., Keesara, V.R. and Sridhar, V. 2021.** Analysis of land use and land cover using machine learning algorithms on google earth engine for Munneru river basin, India. *Sustainability* (Switzerland), **13**(24). 15 pp. doi: 10.3390/su132413758
- Lu, D., Mausel, P., Brondízio, E. and Moran, E. 2004.** Change detection techniques. *International Journal of Remote Sensing*, **25**(12). 2365–2401. doi: 10.1080/0143116031000139863
- Mahabir, D. and Nurse, L. 2007.** *An assessment of the vulnerability of the Cocal area, Manzanilla, Trinidad, to coastal erosion and projected sea level rise and some implications for land use. CERMES Technical Report No. 4*, 49 pp.
- Mahdianpari, M., Salehi, B., Rezaee, M., Mohammadimanesh, F. and Zhang, Y. 2018.** Very deep convolutional neural networks for complex land cover mapping using multispectral remote sensing imagery. *Remote Sensing*, **10**(7). 21 pp. doi: 10.3390/rs10071119
- Manandhar, R., Odeh, I. and Ancev, T. 2009.** Improving the Accuracy of Land Use and Land Cover Classification of Landsat Data Using Post-Classification Enhancement. *Remote Sensing*, **1**(3). 330–344. doi: 10.3390/rs1030330
- Martínez-Megías, C. and Rico, A. 2022.** Biodiversity impacts by multiple anthropogenic stressors in Mediterranean coastal wetlands. *Science of the Total Environment*, **818**. 13 pp. doi: <https://doi.org/10.1016/j.scitotenv.2021.151712>
- Mashala, M.J., Dube, T., Mudereri, B.T., Ayisi, K.K. and Ramudzuli, M.R. 2023.** A Systematic Review on Advancements in Remote Sensing for Assessing and Monitoring Land Use and Land Cover Changes Impacts on Surface Water Resources in Semi-Arid Tropical Environments. *Remote Sensing*, **15**(16). 29 pp. doi: 10.3390/rs15163926
- Millán, S., Rodríguez-Rodríguez, J. and Paula, S.-C. 2021.** Delimitation and classification of coastal wetlands: Implications for the environmental management of the Colombian Continental Caribbean. *Bulletin of Marine and Coastal Research*, **50**(1), 121–140.
- Murdiyarso, D., Purbopuspito, J., Kauffman, J.B., Warren, M.W., Sasmito, S.D., Donato, D.C., Manuri, S., Krisnawati, H., Taberima, S. and Kurnianto, S. 2015.** The potential of Indonesian mangrove forests for global climate change mitigation. *Nature Climate Change*, **5**(12), 1089–1092. doi: 10.1038/nclimate2734
- Nandy, S., Lal, P., Kuppasamy, S., Bagaria, P., Ii, S.N., Debashish, M.I. and Sivakumar, K. 2017.** Application of different satellite image classification techniques for mapping land use and land cover of East Godavari River estuarine landscape Andhra Pradesh, India. *International Journal of Advancement in Remote Sensing*, **5**(1), 37–52
- Newton, A., Icely, J., Cristina, S., Perillo, G.M.E., Turner, R.E., Ashan, D., Cragg, S., Luo, Y., Tu, C., Li, Y., Zhang, H., Ramesh, R., Forbes, D.L.,**

- Solidoro, C., Béjaoui, B., Gao, S., Pastres, R., Kelsey, H., Taillie, D. and Kuenzer, C. 2020.** Anthropogenic, direct pressures on coastal wetlands. *Frontiers in Ecology and Evolution*, **8**. 29 pp. <https://doi.org/10.3389/fevo.2020.00144>
- Nie, X., Jin, X., Wu, J., Li, W., Wang, H. and Yao, Y. 2023.** Evaluation of coastal wetland ecosystem services based on modified choice experimental model: a case study of mangrove wetland in Beibu Gulf, Guangxi. *Habitat International*, **131**. 27 pp. <https://doi.org/10.1016/j.habitatint.2022.102735>
- Odindi, J., Adam, E., Ngubane, Z., Mutanga, O. and Slotow, R. 2014.** Comparison between WorldView-2 and SPOT-5 images in mapping the bracken fern using the random forest algorithm. *Journal of Applied Remote Sensing*, **8**(1). 17 pp. doi: 10.1117/1.JRS.8.083527
- Olaf, R., Philipp F. and Thomas B. 2015.** U-Net: Convolutional networks for biomedical image segmentation. *Medical Image Computing and Computer-Assisted Intervention*, **9351**. 8 pp.
- Patil, A. and Panhalkar, S. 2023.** Comparative analysis of machine learning algorithms for land use and land cover classification using google earth engine platform. *Journal of Geomatics*, **17**(2), 111–118. doi: 10.58825/jog.2023.17.2.96
- Paul A.L. and Sambran C. 2022.** Flooding leaves disaster zone in Manzanilla/Mayaro. Retrieved from <https://www.guardian.co.tt/news/flooding-leaves-disaster-zone-in-manzanillamayaro-6.2.1575132.6e3e3d7d64>
- Pham, L.H., Pham, L.T.H., Dang, T.D., Tran, D.D. and Dinh, T.Q. 2022.** Application of Sentinel-1 data in mapping land-use and land cover in a complex seasonal landscape: a case study in coastal area of Vietnamese Mekong Delta. *Geocarto International*, **37**(13), 3743–3760. doi: 10.1080/10106049.2020.1869329
- Qian, Y., Zhou, W., Yan, J., Li, W. and Han, L. 2014.** Comparing machine learning classifiers for object-based land cover classification using very high resolution imagery. *Remote Sensing*, **7**(1), 153–168. doi: 10.3390/rs70100153
- Roopnarine, C., Ramlal, B. and Roopnarine, R. 2022.** A comparative analysis of weighting methods in geospatial flood risk assessment: a Trinidad case study. *Land*, **11**(10). 30 pp. doi: 10.3390/land11101649
- Rozenstein, O. and Karnieli, A. 2011.** Comparison of methods for land-use classification incorporating remote sensing and GIS inputs. *Applied Geography*, **31**(2), 533–544. doi: 10.1016/j.apgeog.2010.11.006
- Saah, D., Tenneson, K., Matin, M., Uddin, K., Cutter, P., Poortinga, A., Nguyen, Q.H., Patterson, M., Johnson, G., Markert, K., Flores, A., Anderson, E., Weigel, A., Ellenberg, W.L., Bhargava, R., Aekakkararungroj, A., Bhandari, B., Khanal, N., Housman, I.W. and Chishtie, F. 2019.** Land cover mapping in data scarce environments: challenges and opportunities. *Frontiers in Environmental Science*, **7**. 11 pp. doi: 10.3389/fevs.2019.00150
- Soanes, L.M., Pike, S., Armstrong, S., Creque, K., Norris-Gumbs, R., Zaluski, S. and Medcalf, K. 2021.** Reducing the vulnerability of coastal communities in the Caribbean through sustainable mangrove management. *Ocean and Coastal Management*, **210**(3). 15 pp. doi: 10.1016/j.ocecoaman.2021.105702
- Stewart, A., Seepersad, C., Hosein, A., Tripathi, V., Mohammed, A., Agard, J., Cashman, A., Chadee, D. and Ramsuhag, A. 2022.** Water Poverty Indices of three rural communities in the southern Caribbean. *Water Supply*, **22**(3), 3158–3177. doi: 10.2166/ws.2021.409
- Talukdar, S., Singha, P., Mahato, S., Shahfahad, Pal, S., Liou, Y.A. and Rahman, A. 2020.** Land-use land-cover classification by machine learning classifiers for satellite observations-a review. *Remote Sensing*, **12**(7). 22 pp. MDPI AG. doi: 10.3390/rs12071135
- Thakur, P.K., Samant, S.S., Verma, R.K., Saini, A. and Chauhan, M. 2024.** Monitoring forest cover changes and its impact on land surface temperature using geospatial technique in Talra Wildlife Sanctuary, Shimla, India. *Environment, Development and Sustainability*, **26**. 21 pp. doi: 10.1007/s10668-023-04347-x
- Thinh, T. Van, Duong, P.C., Nasahara, K.N. and Tadono, T. 2019.** How does land use/land cover map's accuracy depend on number of classification classes? *SOLA*, **15**, 28–31. doi: 10.2151/sola.2019-006
- Vali, A., Comai, S. and Matteucci, M. 2020.** Deep learning for land use and land cover classification based on hyperspectral and multispectral earth observation data: a review. *Remote Sensing*, **12**(15), 31 pp. doi: 10.3390/rs12152495
- Vizzari, M. 2022.** PlanetScope, Sentinel-2, and Sentinel-1 data integration for object-based land cover classification in Google Earth Engine. *Remote Sensing*, **14**(11), 19 pp. doi: 10.3390/rs14112628
- Wang, X., Gao, X., Zhang, Y., Fei, X., Chen, Z., Wang, J., Zhang, Y., Lu, X. and Zhao, H. 2019.** Land-cover classification of coastal wetlands using the RF algorithm for Worldview-2 and Landsat 8 images. *Remote Sensing*, **11**(16), 22 pp. doi: 10.3390/rs11161927
- Zhao, Z., Islam, F., Waseem, L.A., Tariq, A., Nawaz, M., Islam, I.U., Bibi, T., Rehman, N.U., Ahmad, W., Aslam, R.W., Raza, D. and Hatamleh, W.A. 2024.** Comparison of three machine learning algorithms using Google Earth Engine for Land Use Land Cover Classification. *Rangeland Ecology & Management*, **92**, 129–137. doi: 10.1016/j.rama.2023.10.007
- Zhu, Z., Qiu, S. and Ye, S. 2022.** Remote sensing of land change: A multifaceted perspective. *Remote Sensing of Environment*, **282**, 20 pp. doi: 10.1016/j.rse.2022.113266